Virology 502 (2017) 33–38

Contents lists available at ScienceDirect

Virology

journal homepage: www.elsevier.com/locate/yviro

Porcine deltacoronavirus nsp5 inhibits interferon-β production through the cleavage of NEMO

Xinyu Zhu[a,c], Liurong Fang[a,c], Dang Wang[a,c,*], Yuting Yang[a,c], Jiyao Chen[a,c], Xu Ye[a,c], Mohamed Frahat Foda[a,b], Shaobo Xiao[a,c,*]

[a] State Key Laboratory of Agricultural Microbiology, College of Veterinary Medicine, Huazhong Agricultural University, Wuhan 430070, China
[b] Department of Biochemistry, Faculty of Agriculture, Benha University, Moshtohor, Toukh 13736, Egypt
[c] The Cooperative Innovation Center for Sustainable Pig Production, Wuhan 430070, China

ARTICLE INFO

Keywords:
Porcine deltacoronavirus
nsp5
3C-like protease
Interferon-β
NEMO

ABSTRACT

Porcine deltacoronavirus (PDCoV) causes acute enteric disease and mortality in seronegative neonatal piglets. Previously we have demonstrated that PDCoV infection suppresses the production of interferon-beta (IFN-β), while the detailed mechanisms are poorly understood. Here, we demonstrate that nonstructural protein 5 (nsp5) of PDCoV, the 3C-like protease, significantly inhibits Sendai virus (SEV)-induced IFN-β production by targeting the NF-κB essential modulator (NEMO), confirmed by the diminished function of NEMO cleaved by PDCoV. The PDCoV nsp5 cleavage site in the NEMO protein was identified as glutamine 231, and was identical to the porcine epidemic diarrhea virus nsp5 cleavage site, revealing the likelihood of a common target in NEMO for coronaviruses. Furthermore, this cleavage impaired the ability of NEMO to activate the IFN response and downstream signaling. Taken together, our findings reveal PDCoV nsp5 to be a newly identified IFN antagonist and enhance the understanding of immune evasion by deltacoronaviruses.

1. Introduction

Porcine deltacoronavirus (PDCoV), a new swine enteropathogenic coronavirus, belongs to the genus Deltacoronavirus in the family Coronaviridae (Woo et al., 2009, 2012). It is an enveloped virus with a single-stranded, positive-sense RNA genome of nearly 25 kb, initially detected in pigs in Hong Kong, China in 2012 (Woo et al., 2012). The clinical significance of PDCoV has been highlighted since outbreaks of this virus, which causes severe diarrhea and mortality of piglets, occurred in multiple states of the United States in 2014 (Chen et al., 2015; Homwong et al., 2016; Hu et al., 2015, 2016; Jung et al., 2015; Ma et al., 2015; Marthaler et al., 2014; Thachil et al., 2015). Subsequently, reports of PDCoV in China, South Korea and Canada have caused considerable attention to be paid to the strategy employed by this emerging coronavirus to manipulate the host immune response (Dong et al., 2015; Lee et al., 2016).

The interferons (IFNs) are vital proteins in innate immune signaling, playing a key role in the initial stages of virus invasion. Through the recognition of pathogen-associated molecular patterns by pattern recognition receptors, such as cytoplasmic RIG-I and MDA5, adapter molecules such as IPS-1 can be recruited and subsequently transfer the signal to the IKKα, IKKβ, IKKγ (also called NF-κB essential modulator (NEMO)), TBK1 and IKK-ε. As an essential adapter, NEMO is responsible for the recruitment of TBK1 and IKKε and the activation of IKK complex, leading to the triggering and transportation of NF-κB and IRF3 to the nucleus, both of which induce downstream IFN-β production (Kawai and Akira, 2006; Loo and Gale, 2011; Ramos and Gale, 2011; Seth et al., 2005; Yoneyama and Fujita, 2009).

Notably, recent studies have demonstrated that several viral proteins encoded by coronaviruses (CoV), such as severe acute respiratory syndrome (SARS) CoV, Middle East respiratory syndrome CoV and mouse hepatitis virus, can modulate innate antiviral signaling (Li et al., 2016; Lui et al., 2016; Thornbrough et al., 2016). Relying on its proteinase activity, CoV non-structural protein 5 (nsp5), also called 3C-like protease or main protease, is responsible for processing the viral polyprotein to produce most of the non-structural proteins during viral replication (Lai and Cavanagh, 1997; Masters, 2006; Perlman and Netland, 2009; Ziebuhr et al., 2000). The 3C-like protease of the Arterivirus porcine reproductive and respiratory syndrome virus (PRRSV), and the 3 C proteases of foot-and-mouth disease virus (FMDV) and hepatitis A virus (HAV), both of which belong to the Picornaviridae family, are reported to impair innate immune signaling (Huang et al., 2014; Wang et al., 2012, 2014). A study published by our lab also demonstrated that nsp5, the 3C-like protease of porcine

* Correspondence to: College of Veterinary Medicine, Huazhong Agricultural University, 1 Shi-zi-shan Street, Wuhan 430070, China.
E-mail addresses: wangdang511@126.com, wangdang@mail.hzau.edu.cn (D. Wang), vet@mail.hzau.edu.cn (S. Xiao).

http://dx.doi.org/10.1016/j.virol.2016.12.005
Received 18 October 2016; Received in revised form 30 November 2016; Accepted 3 December 2016

epidemic diarrhea virus (PEDV), which is classified into the Alphacoronavirus family, antagonizes IFN-β production by cleavage of NEMO (Wang et al., 2016). Recently, our research has shown that infection with PDCoV inhibits RIG-I-mediated IFN signaling, although the specific inhibition mechanism remains poorly understood (Luo et al., 2016). As such, we were extremely interested to discover whether nsp5 of PDCoV could disrupt type I IFN signaling.

In this study, we reveal that nsp5 of PDCoV antagonizes the type I IFN signaling pathway through the cleavage of NEMO, a critical constituent of the IKK complex, thus representing a newly identified mechanism by which PDCoV evades the innate immune response.

2. Materials and methods

2.1. Cells, viruses, and reagents

Human embryonic kidney cells (HEK-293T) and porcine kidney cells (PK-15) were obtained from the China Center for Type Culture Collection. LLC-PK1 cells for PDCoV infection were purchased from the ATCC (ATCC number CL-101) and cultured at 37 °C in 5% CO2 in Dulbecco's Modified Eagle's medium (Invitrogen, USA) supplemented with 10% fetal bovine serum. PDCoV strain CHN-HN-2014 (GenBank number KT336560) isolated from a suckling piglet with severe diarrhea in China in 2014, was the object of this research (Dong et al., 2016). Sendai virus (SEV) was acquired from the Center of Virus Resource and Information at the Wuhan Institute of Virology.

2.2. Plasmids and luciferase reporter gene assay

The utilized luciferase reporter plasmids of IFN-β-Luc, NF-κB-Luc and IRF3-Luc have been previously described (Wang et al., 2008, 2010). The RIG-I, IPS1, MDA5, NEMO, and the activated mutant of NEMO (NEMO-K277A) expression plasmids were constructed as previously described (Wang et al., 2008, 2010, 2012). NEMO and its mutants were cloned into the plasmid pCAGGS-Flag with an N-terminal Flag tag (Wang et al., 2012, 2014, 2016). PDCoV nsp5 was amplified and cloned with a C-terminal hemagglutinin (HA) tag into the expression plasmid pCAGGS-HA-C.

Reporter and various expression plasmids were transfected into HEK-293T cells or PK-15 cells in 24-well plates. Twenty-four hours after transfection, cells were stimulated for 16 h with SEV. Firefly luciferase and renilla luciferase activities of lysed cells were verified with a luciferase reporter assay system (Promega, Madison, WI), and normalized to pRL-TK (Promega).

2.3. RNA extraction and quantitative real-time PCR

TRIzol reagent (Invitrogen) and avian myeloblastosis virus reverse transcriptase (TaKaRa, Japan) were utilized for RNA extraction and reverse transcription of cDNA. Each quantitative real-time PCR (qPCR) experiment, evaluated by SYBR green, was performed three times and normalized with glyceraldehyde-3-phosphate dehydrogenase (GAPDH). Primers used for qPCR are detailed in Table 1.

2.4. Western blotting

In western blot analyses, 30 h after transfection, the cells were treated with lysis buffer (Beyotime, China) in 60-mm dishes. The lysates were separated by SDS-PAGE and transferred to polyvinylidene difluoride membranes (Millipore, USA). Following this, an anti-Flag antibody (Macgene, China), was applied to analyze the expression of proteins such as RIG-I, MDA5, IPS-1, and NEMO. PDCoV nsp5 and its mutant were tested with an anti-HA antibody (MBL, Japan) in western blot analyses. The endogenous NEMO in PDCoV-infected cells was tested with an anti-NEMO polyclonal antibody (ABclonal, China). The expression of PDCoV N-protein was assessed with an anti-PDCoV N-protein monoclonal antibody (Luo et al., 2016). The anti-β-actin mouse monoclonal antibody (Beyotime, China) was applied to distinguish the expression of β-actin and to determine equal loading of each sample.

Table 1
Primers used for real-time PCR.

Primer	Sequences (5′ to 3′)
NEMO-F	TACCACCAGCTTTTCCAGGA
NEMO-R	CTCCTCCTTCAGCTTGTCGA
OAS1-F	AAGCATCAGAAGCTTTGCATCTT
OAS1-R	CAGGCCTGGGTTTCTTGAGTT
ISG54-F	CTGGCAAAGAGCCCTAAGGA
ISG54-R	CTCAGAGGGTCAATGGAATTCC
ISG56-F	AAATGAATGAAGCCCTGGAGTATT
ISG56-R	AGGGATCAAGTCCCACAGATTTT
MX1-F	GGCGTGGGAATCAGTCATG
MX1-R	AGGAAGGTCTATGAGGGTCAGA
RANTES-F	ACACCCTGCTGTTTTTCCTAC
RANTES-R	AGACGACTGCTGCCATGGA
SEV HN-F	AAAATTACATGGCTAGGAGGGAAAC
SEV HN-R	GTGATTGGAATGGTTGTGACTCTTA
GAPDH-F	ACATGGCCTCCAAGGAGTAAGA
GAPDH-R	GATCGAGTTGGGGCTGTGACT

3. Results and discussion

3.1. PDCoV nsp5 suppresses IFN-β promoter activation

Coronavirus nsp5 plays an indispensable role in viral replication and immunoregulation. To characterize PDCoV nsp5 with regards to type I IFN signaling, we constructed an expression vector encoding the nsp5 of PDCoV and determined its impact on SEV-induced IFN-β synthesis. Firstly, the cytotoxicity of PDCoV nsp5 in transiently transfected PK-15 and HEK-293T cells was evaluated using the methylthiazolyldiphenyl-tetrazolium bromide (MTT) assay. As shown in Fig. 1A and Fig. 1B, no detectable cytotoxicity could be observed in cells transfected with nsp5 expression plasmid equal to or less than 1.0 μg in 24-well cell culture plates. Further, the data presented in Fig. 1C and D revealed that nsp5 exhibited strong inhibition of SEV-induced IFN-β promoter activity in both cell types. The SEV-induced IFN-β protein in the supernatant was also strongly decreased under the ectopic expression of PDCoV nsp5 in HEK-293T cells (Fig. 1E). Moreover, nsp5 inhibited the activity of both IRF3 and NF-κB-dependent promoters in a dose-dependent manner (Fig. 1F and G). These data revealed the antagonistic role of PDCoV nsp5 in type I IFN signaling.

As the nsp5 of CoV contains the catalytic residue Cys144, a point mutation here could disrupt protease activity (Anand et al., 2003; Hsu et al., 2005; Ye et al., 2016). Consistent with this, sequence alignment showed that Cys144 (numbering based on PDCoV nsp5) residues are highly conserved among other CoV subfamilies (Fig. 2A). Conversely to the activity of wild-type PDCoV nsp5, the activity of SEV-induced IFN-β promoter was strongly restored upon the overexpression of nsp5 C144A (Fig. 2B), implying that the protease activity of PDCoV nsp5 participated in IFN-β antagonism.

3.2. PDCoV nsp5 cleaves NEMO to disrupt RIG-I/MDA5 signaling

To verify at which point in the signaling cascade nsp5 facilitated its inhibitory role, we assessed several crucial molecules in the MDA5/RIG-I signaling pathway, which play an important role in induction of IFN-β production (Yoneyama and Fujita, 2007), including RIG-I, MDA5, IPS-1, NEMO, and TBK1. Similar to previous studies, over-expression of these crucial molecules significantly activated the IFN-β promoter compared with cells transfected with the empty vector control (Siu et al., 2014; Wang et al., 2012, 2016). However, PDCoV

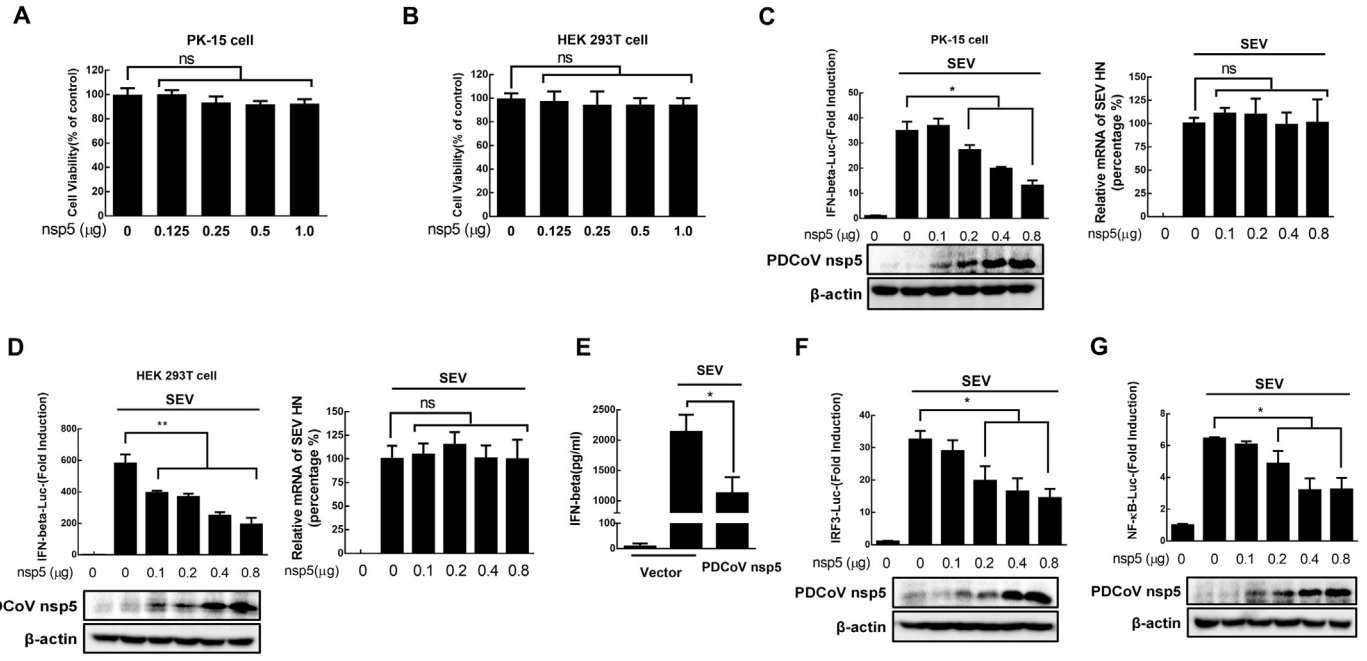

Fig. 1. Porcine deltacoronavirus (PDCoV) nsp5 suppresses IFN-β promoter activation. (A and B) PK-15 cells (A) or HEK-293T cells (B) cultured in 24-well plates were transfected with PDCoV nsp5 expression plasmids and the cell viability was measured by the MTT assay. (C and D) PK-15 cells (C) or HEK-293T cells (D) cultured in 24-well plates were transfected with PDCoV nsp5 expression plasmids along with IFN-β-Luc plasmid and pRL-TK plasmid. The cells were stimulated with 10 hemagglutination units/well of SEV at 24 h after transfection. Sixteen hours later, the cells were harvested for luciferase assays. SEV Haemagglutinin/Neuraminidase (HN) RNA was detected by quantitative RT-PCR. (E) PDCoV nsp5 expression plasmid or empty vector was transfected into HEK-293T cells. The cells were stimulated with 10 hemagglutination units/well of SEV at 24 h after transfection. Sixteen hours post-infection, the supernatants were collected to analyze the expression intensity of IFN-β by ELISA. (F and G) HEK-293T cells were transfected with PDCoV nsp5 along with reporter plasmid IRF3-Luc (F) or NF-κB-Luc (G), followed by stimulation and harvest as described in Fig. 1D.

nsp5 notably impaired the activation of the IFN-β promoter upon stimulation by RIG-I, MDA5, IPS-1 and NEMO. In contrast, TBK1-induced activation of the IFN-β promoter was not affected by nsp5 (Fig. 3A), suggesting that PDCoV nsp5 inhibits RIG-I/MDA5 signaling by targeting NEMO or other upstream proteins. Due to the indispensable role of PDCoV nsp5 protease activity in IFN-β antagonism, we speculated that PDCoV nsp5 cleaved NEMO or an upstream molecule to impair type I IFN signaling. Thus, RIG-I, MDA5, IPS-1 or NEMO were co-transfected with nsp5 into HEK-293T cells. Western blotting showed a smaller band (~24 kDa) in the NEMO/PDCoV nsp5 co-expression samples, while no similar cleavage products were detected with RIG-I, MDA5 or IPS-1 co-transfections (Fig. 3B). Furthermore, the cleavage of NEMO increased gradually with increasing transfection dose of PDCoV nsp5 (Fig. 3C) and the cleaved product could not be observed following transfection with the nsp5 C144A mutant lacking protease activity (Fig. 3D). These data indicate that PDCoV nsp5, relying on its protease activity, targets the essential molecule NEMO for cleavage.

In order to evaluate the real effect of this cleavage on endogenous NEMO protein in viral infection, LLC-PK1 cells were infected with PDCoV at a multiplicity of infection of 0.1 and harvested at 6 h, 12 h, and 24 h post-infection. The results in Fig. 3E indicate that endogenous NEMO was clearly reduced within 6 h of infection and the reduction in NEMO correlated with the duration of PDCoV infection. However, no difference was detected in NEMO mRNA levels between mock- and PDCoV-infected cells at any time during infection (Fig. 3F). The above results indicate that degradation of NEMO occurs only in PDCoV infection, without affecting transcription.

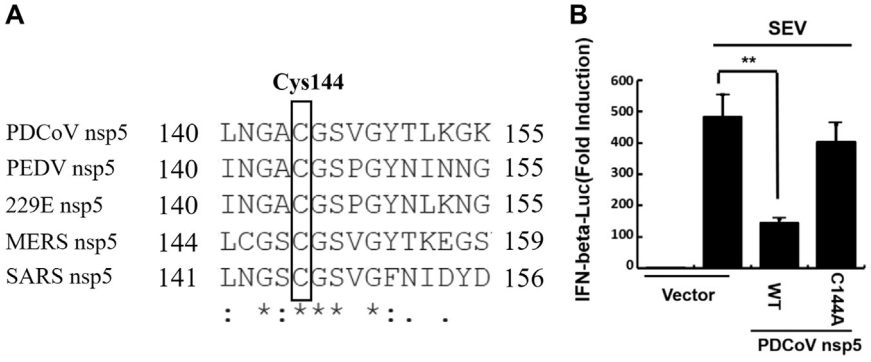

Fig. 2. Protease activity dominates the ability of PDCoV nsp5 to inhibit IFN-β promoter activation. (A) Amino acid alignment of the conserved fragment neighboring Cys144 of nsp5 (established on PDCoV nsp5) in CoV. The amino acid sequences were from GenBank entries with the following accession numbers: PDCoV, ALS54085.1; Porcine epidemic diarrhea virus (PEDV), AFQ37597.1; human coronaviruses 229E (HCoV 229E), AGW80947.1; Middle East respiratory syndrome coronavirus (MERS-CoV), AGV08401.1; severe acute respiratory syndrome coronavirus (SARS-CoV), NP_828850.1. They were analyzed using the website (http://www.ebi.ac.uk/Tools/msa/clustalo/). (B) HEK-293T cells were transfected with expression plasmids encoding PDCoV nsp5 or its protease-defective mutant C144A, for analyzing IFN-β promoter activity followed by stimulation and harvest as described in Fig. 1D. ns, $P > 0.05$; *, $P < 0.05$; **, $P < 0.01$; ***, $P < 0.001$.

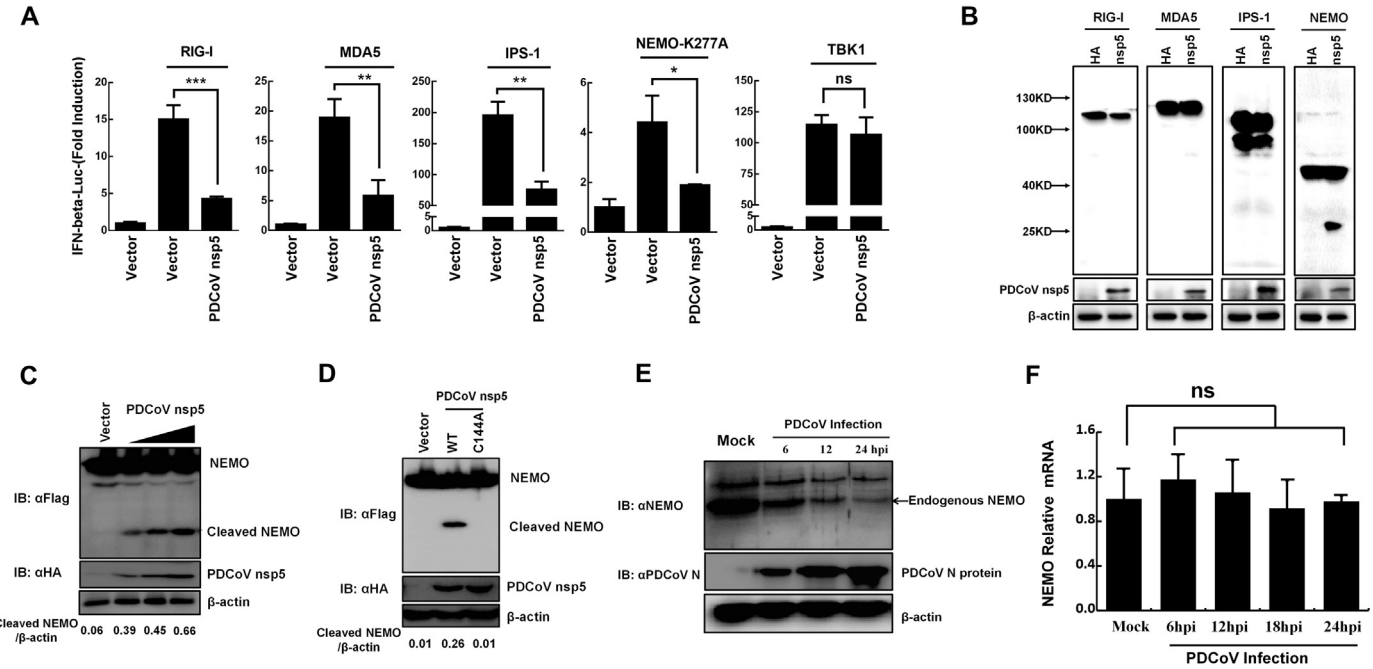

Fig. 3. PDCoV nsp5 cleaves NEMO to disrupt RIG-I/MDA5 signaling. (A) HEK-293T cells were co-transfected with RIG-I, MDA5, IPS-1, NEMO-K277A, or TBK1 expression plasmids along with IFN-β-Luc plasmid, pRL-TK plasmid and PDCoV nsp5. The cells were lysed for luciferase assays at 30 h after transfection. (B) PDCoV nsp5 expression plasmid or an empty vector was transfected with Flag-appended RIG-I, MDA5, IPS-1, or NEMO expression plasmids into HEK-293T cells. The cells were lysed for Western blotting at 32 h after transfection. (C) Flag-appended NEMO expression plasmid and increasing doses of HA-appended PDCoV nsp5 were transfected into HEK-293T cells. The cells were lysed for Western blotting at 32 h after transfection. The relative level of cleaved NEMO was quantified by ImageJ. (D) Wild-type PDCoV nsp5 or its protease-defective mutant (C144A) and NEMO expression plasmid were co-transfected and treated as described in panel B. The relative level of cleaved NEMO was quantified by ImageJ. (E) LLC-PK1 cells were infected with PDCoV strain CHN-HN-2014 and the cells were lysed for Western blotting at different times post-infection. (F) LLC-PK1 cells were infected with PDCoV as described in panel E, harvested at different times post-infection and analyzed for NEMO mRNA levels by qPCR, using SYBR green. ns, $P > 0.05$; *, $P < 0.05$; **, $P < 0.01$; ***, $P < 0.001$.

3.3. PDCoV nsp5 cleaves the glutamine 231 (Q231) of NEMO

The specific preference for substrate cleavage by CoV nsp5 has been previously reported as glutamine (Q) at the P1 position (Chuck et al., 2010, 2011). As such, we examined the P1 position residue of NEMO recognized by PDCoV nsp5. Considering the 24 kDa molecular weight of the cleaved product (N-terminal), a series of NEMO mutants were constructed between amino acids 210 and 263 (Fig. 4A). The WT or mutated NEMO proteins were co-transfected into HEK-293T cells with PDCoV nsp5. The results indicated that Q218A, Q236A/Q239A or Q259A mutations were cleaved by PDCoV nsp5 normally, while Q229A or Q231A mutations was resistant to cleavage (Fig. 4B). As previously found, the common substrate preference of CoV nsp5 consists of leucine (L) at the P2 position and glutamine, lysine (K) or isoleucine (I), all of which contain a long side-chain and positive charge, at the P3 position (Chuck et al., 2010, 2011; Wang et al., 2016). We speculated that if Q231 is the P1 residue, then the recognition and cleavage of Q231 by PDCoV nsp5 could be affected by a Q229A mutation (Fig. 4C). Therefore, two Q229 mutants at the speculated P3 position were substituted with lysine or arginine (R) which also has a long side-

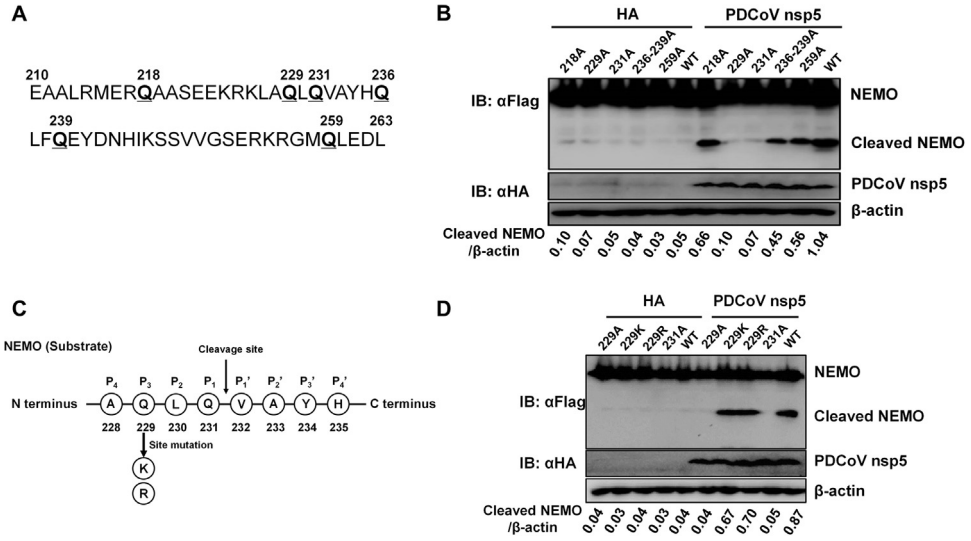

Fig. 4. PDCoV nsp5 cleaves the glutamine 231 (Q231) of NEMO. (A) Schematic diagram of NEMO mutants. (B) HEK-293T cells were transfected with PDCoV nsp5 and WT NEMO or NEMO mutants as indicated. Cells were lysed at 32 h after transfection and analyzed by Western blotting. (C) Schematic illustration of the NEMO cleavage site by PDCoV nsp5. (D) PDCoV nsp5 and WT NEMO or NEMO mutants were transfected as described in panel B. The relative level of cleaved NEMO was quantified by ImageJ.

chain and positive charge. Evidently, Q229K and Q229R mutation can be cleaved to produce the same cleavage product as WT NEMO (Fig. 4D), revealing that Q231, but not Q229, is the P1 position residue cleaved by PDCoV nsp5. Docking studies between CoV nsp5 and substrate showed that through van der Waals interactions, the side chain of P3 residues could interact with the side chain of glutamic acid at residue 164 (Xue et al., 2008). The homology model for PEDV nsp5 and the NEMO peptide substrate also illustrated that a long side chain in the P3 position strongly supported nsp5–substrate recognition (Wang et al., 2016). These studies provide important clues for the PDCoV nsp5–NEMO interaction and give a possible explanation for the finding that mutant Q229A, but not Q229K or Q229R, significantly impaired cleavage by PDCoV nsp5.

3.4. PDCoV nsp5-mediated NEMO cleavage limits the activation of type I IFN signaling

To assess the influence of NEMO cleavage by PDCoV nsp5 in type I IFN signaling, a constitutively active NEMO mutant, NEMO-K277A, was used, leading to more efficient activation of the IFN-β promoter compared with WT NEMO (Bloor et al., 2008; Wang et al., 2016, 2014). The K277A mutation has the same cleavage site as WT NEMO, with the PDCoV nsp5 P1 recognition site also being Q231 (Fig. 5A). Hence, the IFN-β promoter activated by NEMO-K277A, was suppressed by PDCoV nsp5 in a dose-dependent manner and this suppression was lost upon the expression of the protease-defective nsp5 C144A mutant (Fig. 5B and C).

To evaluate the activity of the cleavage fragment in activation of the IFN response, NEMO-K277A (1-231AA), NEMO-K277A (232-419AA) or NEMO-K277A (full) expression plasmids were transfected into PK-15 cells. Quantitative PCR showed that mRNA levels of immune-related molecules, such as ISG54, ISG56, MX1, OAS1, and RANTES, were not successfully induced by the cleaved fragments of 1–231 or 232–419 (Fig. 5D). A previous study of PEDV nsp5 showed that cleavage fragments of NEMO did not activate IFN-β, IRF3 or NF-κB-dependent promoters (Wang et al., 2016). As the cleavage site Q231 is identical for both PEDV and PDCoV nsp5, these results together demonstrate that PDCoV nsp5-induced cleavage fragments lack the capacity to activate the type I IFN response and downstream signaling, revealing that the role of NEMO in type I IFN signaling can be significantly inhibited following cleavage by PDCoV nsp5.

So far, evidence presented by recent studies has shown that the 3C and 3C-like proteases of different viruses cleave NEMO at multiple residues, such as Q383 and Q304 targeted by FMDV and HAV 3C proteases, E349 targeted by PRRSV 3C-like proteases and Q231 targeted by PEDV 3C-like protease, leading to disruption of IFN-β production (Huang et al., 2014; Wang et al., 2012, 2016, 2014) and implying that NEMO is a common target easily hijacked by viral proteases. In particular, the conserved Q231 residue recognized by both PDCoV nsp5 and PEDV nsp5 prompted us to speculate that the same IFN antagonistic mechanism may be common to members of the Coronaviridae family. It is worth investigating whether nsp5 from different CoV genera, including Alpha-, Beta-, Gamma-, and Deltacoronaviruses, retain the ability to cleave NEMO and comparing this property between the different CoV genera.

In summary, our research demonstrated that PDCoV nsp5 has the capacity to impede generation of IFN-β. As a new IFN antagonist encoded by a deltacoronavirus, PDCoV nsp5 induced the cleavage of NEMO at the conserved residue Q231, leading to suppression of the type I IFN signaling pathway. Our research provides new insights into strategies and tactics employed by PDCoV in host innate immune evasion.

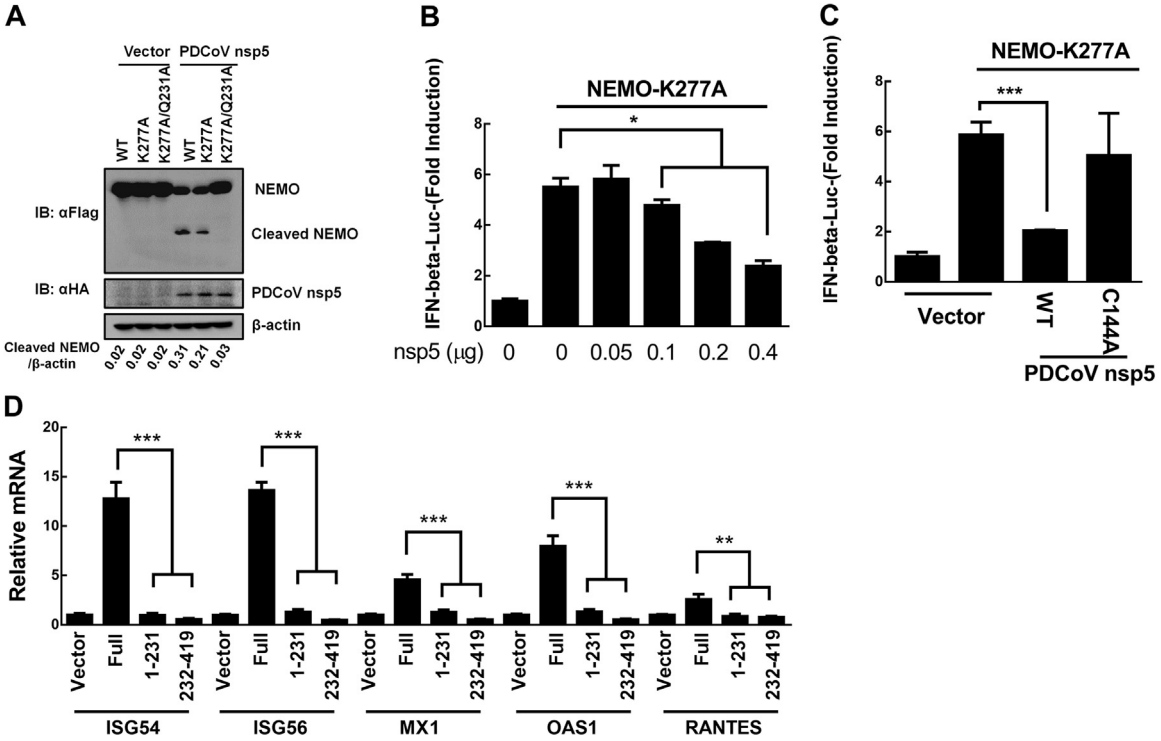

Fig. 5. PDCoV nsp5-mediated NEMO cleavage limits the activation of type I IFN signaling. (A) HEK-293T cells were transfected with WT NEMO, a constitutively activated form of NEMO (NEMO-K277A) or its mutant (NEMO-K277A/Q231A), along with PDCoV nsp5 or empty vector. Cells were lysed at 32 h after transfection and analyzed by Western blotting. The relative level of cleaved NEMO was quantified by ImageJ. (B) HEK-293T cells were transfected with IFN-β-Luc plasmid, pRL-TK plasmid and NEMO-K277A expression plasmid, along with increasing doses of PDCoV nsp5 expression plasmid. Luciferase assays were performed at 30 h after transfection. (C) HEK-293T cells were co-transfected with the reporter plasmid described in panel B along with wild-type PDCoV nsp5 or its mutant losing protease activity (C144A). Luciferase assays were performed at 36 h after transfection. (D) NEMO-K277A (full), NEMO-K277A (1-231AA), NEMO-K277A (232-419AA) or empty vector were transfected into PK-15 cells. After 32 h, PK-15 cells were analyzed for ISG54, ISG56, MX1, OAS1, RANTES mRNA levels in qPCR, using SYBR green. ns, $P > 0.05$; *, $P < 0.05$; **, $P < 0.01$; ***, $P < 0.001$.

Acknowledgements

This work was supported by the National Key R & D Plan of China (2016YFD0500103), the Key Technology R & D Programme of China (2015BAD12B02), the National Natural Science Foundation of China (31672566), and the Natural Science Foundation of Hubei Province (2014CFA009).

References

Anand, K., Ziebuhr, J., Wadhwani, P., Mesters, J.R., Hilgenfeld, R., 2003. Coronavirus main proteinase (3CLpro) structure: basis for design of anti-SARS drugs. Science 300, 1763–1767.

Bloor, S., Ryzhakov, G., Wagner, S., Butler, P.J., Smith, D.L., Krumbach, R., Dikic, I., Randow, F., 2008. Signal processing by its coil zipper domain activates IKK gamma. Proc. Natl. Acad. Sci. USA 105, 1279–1284.

Chen, Q., Gauger, P., Stafne, M., Thomas, J., Arruda, P., Burrough, E., Madson, D., Brodie, J., Magstadt, D., Derscheid, R., Welch, M., Zhang, J., 2015. Pathogenicity and pathogenesis of a United States porcine deltacoronavirus cell culture isolate in 5-day-old neonatal piglets. Virology 482, 51–59.

Chuck, C.P., Chong, L.T., Chen, C., Chow, H.F., Wan, D.C., Wong, K.B., 2010. Profiling of substrate specificity of SARS-CoV 3CL. PLoS One 5, e13197.

Chuck, C.P., Chow, H.F., Wan, D.C., Wong, K.B., 2011. Profiling of substrate specificities of 3C-like proteases from group 1, 2a, 2b, and 3 coronaviruses. PLoS One 6, e27228.

Dong, N., Fang, L., Zeng, S., Sun, Q., Chen, H., Xiao, S., 2015. Porcine Deltacoronavirus in Mainland China. Emerg. Infect. Dis. 21, 2254–2255.

Dong, N., Fang, L., Yang, H., Liu, H., Du, T., Fang, P., Wang, D., Chen, H., Xiao, S., 2016. Isolation, genomic characterization, and pathogenicity of a Chinese porcine deltacoronavirus strain CHN-HN-2014. Vet. Microbiol.. http://dx.doi.org/10.1016/j.vetmic.2016.10.022.

Homwong, N., Jarvis, M.C., Lam, H.C., Diaz, A., Rovira, A., Nelson, M., Marthaler, D., 2016. Characterization and evolution of porcine deltacoronavirus in the United States. Prev. Vet. Med. 123, 168–174.

Huang, C., Zhang, Q., Guo, X.K., Yu, Z.B., Xu, A.T., Tang, J., Feng, W.H., 2014. Porcine reproductive and respiratory syndrome virus nonstructural protein 4 antagonizes beta interferon expression by targeting the NF-kappaB essential modulator. J. Virol. 88, 10934–10945.

Hu, H., Jung, K., Vlasova, A.N., Chepngeno, J., Lu, Z., Wang, Q., Saif, L.J., 2015. Isolation and characterization of porcine deltacoronavirus from pigs with diarrhea in the United States. J. Clin. Microbiol. 53, 1537–1548.

Hu, H., Jung, K., Vlasova, A.N., Saif, L.J., 2016. Experimental infection of gnotobiotic pigs with the cell-culture-adapted porcine deltacoronavirus strain OH-FD22. Arch. Virol. 161, 3421–3434.

Hsu, M.F., Kuo, C.J., Chang, K.T., Chang, H.C., Chou, C.C., Ko, T.P., Shr, H.L., Chang, G.G., Wang, A.H., Liang, P.H., 2005. Mechanism of the maturation process of SARS-CoV 3CL protease. J. Biol. Chem. 280, 31257–31266.

Jung, K., Hu, H., Eyerly, B., Lu, Z., Chepngeno, J., Saif, L.J., 2015. Pathogenicity of 2 porcine deltacoronavirus strains in gnotobiotic pigs. Emerg. Infect. Dis. 21, 650–654.

Kawai, T., Akira, S., 2006. Innate immune recognition of viral infection. Nat. Immunol. 7, 131–137.

Lai, M.M., Cavanagh, D., 1997. The molecular biology of coronaviruses. Adv. Virus Res. 48, 1–100.

Lee, J.H., Chung, H.C., Nguyen, V.G., Moon, H.J., Kim, H.K., Park, S.J., Lee, C.H., Lee, G.E., Park, B.K., 2016. Detection and Phylogenetic Analysis of Porcine Deltacoronavirus in Korean Swine Farms, 2015. Transbound. Emerg. Dis. 63, 248–252.

Li, S.W., Wang, C.Y., Jou, Y.J., Huang, S.H., Hsiao, L.H., Wan, L., Lin, Y.J., Kung, S.H., Lin, C.W., 2016. SARS coronavirus papain-like protease inhibits the TLR7 signaling pathway through removing Lys63-linked polyubiquitination of TRAF3 and TRAF6. Int. J. Mol. Sci., 17.

Loo, Y.M., Gale, M., Jr., 2011. Immune signaling by RIG-I-like receptors. Immunity 34, 680–692.

Lui, P.Y., Wong, L.Y., Fung, C.L., Siu, K.L., Yeung, M.L., Yuen, K.S., Chan, C.P., Woo, P.C., Yuen, K.Y., Jin, D.Y., 2016. Middle East respiratory syndrome coronavirus M protein suppresses type I interferon expression through the inhibition of TBK1-dependent phosphorylation of IRF3. Emerg. Microbes Infect. 5, e39.

Luo, J., Fang, L., Dong, N., Fang, P., Ding, Z., Wang, D., Chen, H., Xiao, S., 2016. Porcine deltacoronavirus (PDCoV) infection suppresses RIG-I-mediated interferon-beta production. Virology 495, 10–17.

Marthaler, D., Raymond, L., Jiang, Y., Collins, J., Rossow, K., Rovira, A., 2014. Rapid detection, complete genome sequencing, and phylogenetic analysis of porcine deltacoronavirus. Emerg. Infect. Dis. 20, 1347–1350.

Masters, P.S., 2006. The molecular biology of coronaviruses. Adv. Virus Res. 66, 193–292.

Ma, Y., Zhang, Y., Liang, X., Lou, F., Oglesbee, M., Krakowka, S., Li, J., 2015. Origin, evolution, and virulence of porcine deltacoronaviruses in the United States. MBio 6, e00064.

Perlman, S., Netland, J., 2009. Coronaviruses post-SARS: update on replication and pathogenesis. Nat. Rev. Microbiol. 7, 439–450.

Ramos, H.J., Gale, M., Jr., 2011. RIG-I like receptors and their signaling crosstalk in the regulation of antiviral immunity. Curr. Opin. Virol. 1, 167–176.

Seth, R.B., Sun, L., Ea, C.K., Chen, Z.J., 2005. Identification and characterization of MAVS, a mitochondrial antiviral signaling protein that activates NF-kappaB and IRF 3. Cell 122, 669–682.

Siu, K.L., Yeung, M.L., Kok, K.H., Yuen, K.S., Kew, C., Lui, P.Y., Chan, C.P., Tse, H., Woo, P.C., Yuen, K.Y., Jin, D.Y., 2014. Middle east respiratory syndrome coronavirus 4a protein is a double-stranded RNA-binding protein that suppresses PACT-induced activation of RIG-I and MDA5 in the innate antiviral response. J. Virol. 88, 4866–4876.

Thachil, A., Gerber, P.F., Xiao, C.T., Huang, Y.W., Opriessnig, T., 2015. Development and application of an ELISA for the detection of porcine deltacoronavirus IgG antibodies. PLoS One 10, e0124363.

Thornbrough, J.M., Jha, B.K., Yount, B., Goldstein, S.A., Li, Y., Elliott, R., Sims, A.C., Baric, R.S., Silverman, R.H., Weiss, S.R., 2016. Middle east respiratory syndrome coronavirus NS4b protein inhibits host RNase L activation. MBio 7, e00258.

Wang, D., Fang, L., Li, T., Luo, R., Xie, L., Jiang, Y., Chen, H., Xiao, S., 2008. Molecular cloning and functional characterization of porcine IFN-beta promoter stimulator 1(IPS-1). Vet. Immunol. Immunopathol. 125, 344–353.

Wang, D., Fang, L., Luo, R., Ye, R., Fang, Y., Xie, L., Chen, H., Xiao, S., 2010. Foot-and-mouth disease virus leader proteinase inhibits dsRNA-induced type Iinterferon transcription by decreasing interferon regulatory factor3/7 in protein levels. Biochem. Biophys. Res. Commun. 399, 72–78.

Wang, D., Fang, L., Li, K., Zhong, H., Fan, J., Ouyang, C., Zhang, H., Duan, E., Luo, R., Zhang, Z., Liu, X., Chen, H., Xiao, S., 2012. Foot-and-mouth disease virus 3C protease cleaves NEMO to impair innate immune signaling. J. Virol. 86, 9311–9322.

Wang, D., Fang, L., Shi, Y., Zhang, H., Gao, L., Peng, G., Chen, H., Li, K., Xiao, S., 2016. Porcine Epidemic Diarrhea virus 3C-like protease regulates its interferon antagonism by cleaving NEMO. J. Virol. 90, 2090–2101.

Wang, D., Fang, L., Wei, D., Zhang, H., Luo, R., Chen, H., Li, K., Xiao, S., 2014. Hepatitis A virus 3C protease cleaves NEMO to impair induction of beta interferon. J. Virol. 88, 10252–10258.

Woo, P.C., Lau, S.K., Huang, Y., Yuen, K.Y., 2009. Coronavirus diversity, phylogeny and interspecies jumping. Exp. Biol. Med. 234, 1117–1127.

Woo, P.C., Lau, S.K., Lam, C.S., Lau, C.C., Tsang, A.K., Lau, J.H., Bai, R., Teng, J.L., Tsang, C.C., Wang, M., Zheng, B.J., Chan, K.H., Yuen, K.Y., 2012. Discovery of seven novel Mammalian and avian coronaviruses in the genus deltacoronavirus supports bat coronaviruses as the gene source of alphacoronavirus and betacoronavirus and avian coronaviruses as the gene source of gammacoronavirus and deltacoronavirus. J. Virol. 86, 3995–4008.

Xue, X., Yu, H., Yang, H., Xue, F., Wu, Z., Shen, W., Li, J., Zhou, Z., Ding, Y., Zhao, Q., Zhang, X.C., Liao, M., Bartlam, M., Rao, Z., 2008. Structures of two coronavirus main proteases: implications for substrate binding and antiviral drug design. J. Virol. 82, 2515–2527.

Ye, G., Deng, F., Shen, Z., Luo, R., Zhao, L., Xiao, S., Fu, Z.F., Peng, G., 2016. Structural basis for the dimerization and substrate recognition specificity of porcine epidemic diarrhea virus 3C-like protease. Virology 494, 225–235.

Yoneyama, M., Fujita, T., 2007. RIG-I family RNA helicases: cytoplasmic sensor for antiviral innate immunity. Cytokine Growth Factor Rev. 18, 545–551.

Yoneyama, M., Fujita, T., 2009. RNA recognition and signal transduction by RIG-I-like receptors. Immunol. Rev. 227, 54–65.

Ziebuhr, J., Snijder, E.J., Gorbalenya, A.E., 2000. Virus-encoded proteinases and proteolytic processing in the Nidovirales. J. Gen. Virol. 81, 853–879.